ROYAL SOCIETY OF CHEMISTRY

PAPER

Check for updates

Chemo- and regio-selective amidation of indoles with isocyanates using borane Lewis acids†

Ayan Dasgupta, [ID] ‡[a] Michael G. Guerzoni, [ID] ‡[a] Nusaybah Alotaibi, [ID] [a] Yara van Ingen, [ID] [a] Kaveh Farshadfar, [ID] [bd] Emma Richards,*[a] Alireza Ariafard [ID] *[c] and Rebecca L. Melen [ID] *[a]

The efficacy of boron-based catalysts has drawn considerable attention from the scientific community due to their relatively low toxicities and high selectivities. Formation of a new carbon–carbon or carbon–nitrogen bond to generate an amide/urea functionality using mild, catalytic reaction protocols has always been an important challenge, as functionalised amides and urea derivatives are important scaffolds in medicinal chemistry. Herein we report a facile and mild catalytic reaction protocol towards the amidation of N-methyl indoles/pyrroles (17 examples, yields up to 58%) using $B(C_6F_5)_3$ (30 mol%). Moreover, our investigation revealed that although catalytic amounts of $B(C_6F_5)_3$ (10 mol%) are efficient towards the N-carboxamidation of unprotected indoles, catalytic BCl_3 (5 mol%) is capable of producing near quantitative yields of the N-carboxamidation products (21 examples, yields up to 95%). In contrast with previous literature reports, the reaction between 2-(alkynyl)anilines and aryl isocyanates using catalytic BCl_3 (5 mol%) afforded N–H inserted products (9 examples, yields up to 71%) chemo-selectively as opposed to the intramolecular hydroamination product. Comprehensive DFT studies have been undertaken to understand the mechanistic details of the N–H functionalisation of indoles.

[a] *Cardiff Catalysis Institute, School of Chemistry, Cardiff University, Main Building, Park Place, Cardiff, CF10 3AT, Cymru/Wales, UK. E-mail: RichardsE10@cardiff.ac.uk, MelenR@cardiff.ac.uk*
[b] *Department of Chemistry, Islamic Azad University, Central Tehran Branch, Poonak, Tehran, 1469669191, Iran*
[c] *School of Physical Sciences, University of Tasmania, Private Bag 75, Hobart, Tasmania 7001, Australia. E-mail: alireza.ariafard@utas.edu.au*
[d] *Research Group of Computational Chemistry, Department of Chemistry and Materials Science, Aalto University, FI-00076 Aalto, Finland*
† Electronic supplementary information (ESI) available. See DOI: https://doi.org/10.1039/d2cy01441f
‡ Both the authors contributed equally.

The activation of small molecules using main group element based catalysts has increased in popularity over the last two decades and opens up new avenues for bond forming reactions that may offer alternative methods towards the synthesis of fine chemicals.[1] Whilst precious transition metal-based catalysts have been largely used, their toxicities and limited abundance cause problems in developing active molecules for applications in food-, agro-, and medicinal-chemistry.[2] The partially filled d-orbitals present in transition metal species can synergistically accept and donate electrons to and from small molecules, resulting in the activation of both polar and inert bonds.[3] Boranes on the other hand only act as an acceptor whereby the presence of an empty p-orbital renders them Lewis acidic and thus able to activate polar, Lewis basic substrates.[4] The ability to finetune the activity, selectivity, and stability of the borane catalyst can be achieved by altering the ligands attached to the central boron atom. In particular, the use of sterically demanding and electron withdrawing perfluoroaryl ligands (*e.g.*, C_6F_5) has been particularly attractive giving highly active and selective catalysts that can be employed in a range of organic reactions.[5]

Methods to functionalise nitrogen-containing heterocycles[6] are an important and ongoing area of research due to their notable biological and medicinally relevant activities (Scheme 1).[7] The introduction of an amide group at the C3 position of an indole can be carried out through amidation reactions using isocyanate derivatives. Extensive studies have been carried out to establish facile synthetic routes to form such functionalised moieties using transition metals, including Pd, Cu, Zn, and Rh.[8] In addition, in 2016, the carbamoylation of 1-methylindole using stoichiometric Me$_2$AlCl was investigated by Hattori and co-workers.[9]

The N1 functionalisation of unprotected indoles with isocyanates to generate urea moieties has also been extensively studied. A range of transition metal catalysts including Pd,[10] Cu,[11] Ru,[12] and Rh (ref. 13) have been used for N-carboxamidation of unprotected indoles through the formation of a new N–C bond. CsOH·H$_2$O has also been employed as an alternative to the transition metal catalysts.[14] In 2017, Camp and co-workers reported the functionalisation of ureas obtained from the reaction between isocyanates and secondary amines using cyrene as a solvent.[15] In both cases,

5982 | *Catal. Sci. Technol.*, 2022, **12**, 5982–5990

This journal is © The Royal Society of Chemistry 2022

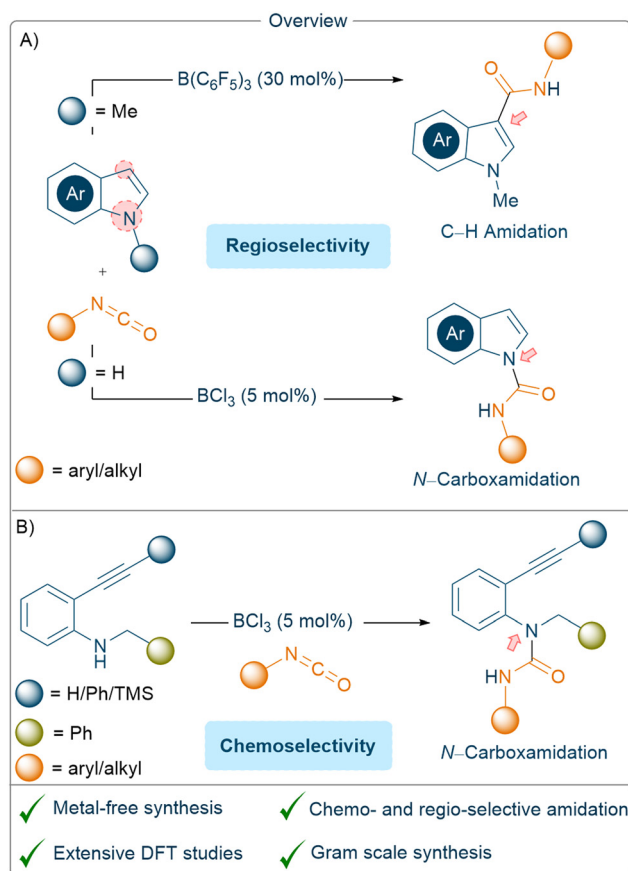**Scheme 1** Medicinally important functionalised urea derivatives.

either the isocyanate scope was limited, or the reaction was only performed with more nucleophilic amines. Strong non-nucleophilic bases, such as NaH, have also been employed in stoichiometric amounts (or a large excess) for the reaction

between unprotected indoles and aryl/alkyl isocyanates to afford urea derivates.[16]

Another route often pursued for the *in situ* generation of indole scaffolds relies on the employment of 2-alkynyl anilines which, upon intramolecular cyclisation, can be further functionalised at the C3 position with various electrophiles. For example, stoichiometric *n*-BuLi in combination with ZnCl$_2$ afforded 3-zinciobenzoheteroles which could be further transformed into C3 Cu complexes and quenched with various electrophiles to afford C3 substituted indole derivatives.[17] In 2017, Paradies and co-workers demonstrated catalytic B(C$_6$F$_5$)$_3$ can be employed for the synthesis of indole derivatives starting from 2-alkynyl anilines. Such intramolecular hydroamination of internal alkynes proceeds through 5-and 6-*endo-dig* cyclisation with proto-deborylation.[18]

In this study, we chose to investigate the regio-and chemo-selective functionalisation of both protected and unprotected indoles with isocyanates using catalytic amounts of borane Lewis acids. We also investigated the reactivities of 2-alkynyl anilines derivatives towards isocyanates using catalytic BCl$_3$ (Scheme 2).

Initially, the borane mediated reaction between 1-methylindole and phenyl isocyanate was examined under various reaction conditions (see ESI† for the optimisation, Table S1). After extensive screening of the borane, solvent, temperature, loading, and time, we found that the optimum conditions for the reaction were 30 mol% B(C$_6$F$_5$)$_3$, trifluorotoluene (TFT) solvent, and 80 °C (Fig. 1, top). Importantly, we could crystallise the product **1b** from the

Scheme 2 An overview of indole amidation reactions: (A); an intramolecular reaction *vs.* N–H insertion of 2-alkynyl anilines, with isocyanates (B).

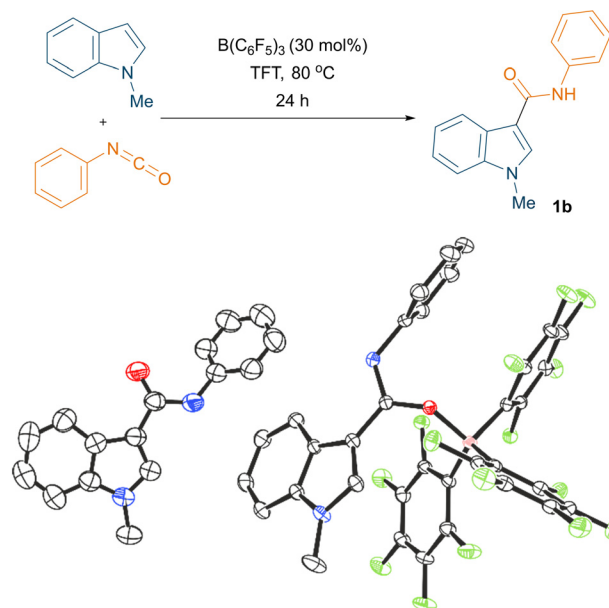**Fig. 1** Reaction of 1-methylindole and phenyl isocyanate (top). Crystal structures of **1b** (bottom left) and **1b**·B(C$_6$F$_5$)$_3$ (bottom right), thermal ellipsoids shown at 50%. H atoms omitted for clarity. Carbon: black; oxygen: red; nitrogen: blue; fluorine: green; boron: pink.
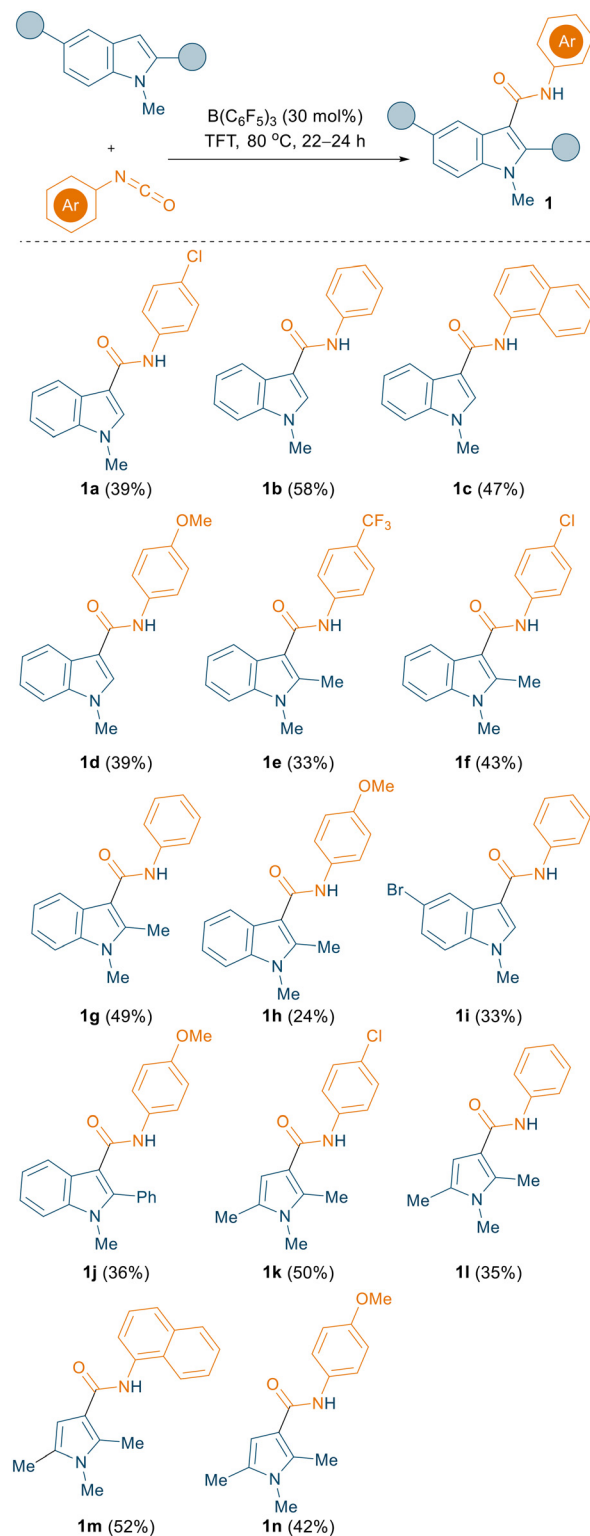
This journal is © The Royal Society of Chemistry 2022

Catal. Sci. Technol., 2022, **12**, 5982–5990 | **5983**

reaction and, when employing stoichiometric B(C₆F₅)₃, the reaction led to the formation of triaryl borane adduct **1b**·B(C₆F₅)₃. Both **1b** and **1b**·B(C₆F₅)₃ could be characterised by single crystal X-ray diffraction (Fig. 1, bottom). Using our optimised reaction conditions, various indole derivatives including 1-methylindole, 1,2-dimethylindole, 5-bromo-1-methylindole, and 1-methyl-2-phenylindole were reacted with aryl isocyanates to afford the corresponding C3 amide substituted products (**1a–1j**) in moderate to good yields (up to 58%, Scheme 3). Interestingly, the reaction between 5-bromo-1-methylindole and 4-chlorophenyl isocyanate did not afford the expected C3 functionalised product.

Instead, slow evaporation from a CH₂Cl₂ solution of two isolated fractions afforded single crystals suitable for X-ray diffraction measurements, which revealed the formation of boron adduct **2** (Fig. S126†) and a C₆F₅-transfer product **3** (see ESI,† Fig. S127) in 39% and 41% yield respectively (Scheme 4, top). We infer that these isolated products, showing catalyst termination, could explain the relatively low yields obtained for other substrates, as well as the high loading of B(C₆F₅)₃ needed for the reaction. This insightful result led us to hypothesise possible further functionalisation of the amidic nitrogen with another molecule of isocyanate. Treatment of compound **1b** with 4-chlorophenyl isocyanate under the optimised conditions pleasingly afforded the *N*-carboxamidated product **4**, albeit in a low yield of 21% (Scheme 4, bottom). Slow evaporation of the solvent from a concentrated ethyl acetate solution of **4** afforded single crystals suitable for X-ray diffraction measurements which confirmed the structure of the product (Fig. S128†).

In addition to indoles, we also investigated the reactivity of aryl isocyanates towards pyrrole substrates. Using the same reaction conditions, 1,2,5-trimethyl-pyrrole was employed for the reaction with various isocyanates to give the corresponding C3 amidation products **1k–1n** in moderate yields (up to 52%, Scheme 3).

During the investigation of the substrate scope, we also examined the reactivities of 2,5-substituted pyrroles with aryl isocyanates. Using our optimised reaction conditions (30 mol% B(C₆F₅)₃, TFT, 80 °C), a mixture of two regio-isomeric products was obtained. Although the C2 amide functionalised products (**1o–1p**, see ESI† Scheme S1) were formed as the major products (yields up to 50%), in each case the C3 functionalised products (**1o′–1p′**, see ESI† Scheme S1) were isolated as minor isomers (yields up to 20%). Due to poor conversion, when 4-methoxy phenyl isocyanate was used, only the C2 functionalised product (**1q**) was isolated in 17% yield.
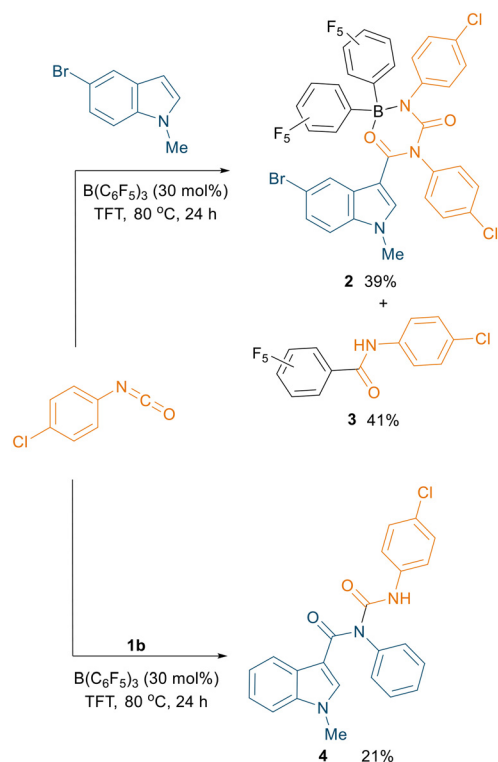
Following the C3 amidation of *N*-protected indoles and pyrroles, we turned our attention to the reactivities of unprotected indoles towards isocyanates. Employing the same reaction conditions used for the C3 C–H amidation of *N*-protected indoles, a reaction between 1*H*-indole and phenyl isocyanate was investigated. In contrast to our above results, NMR (¹H and ¹³C) spectroscopic data clearly indicated the formation of *N*-carboxamidated product **5a** in 17% yield (see

Scheme 3 C3 amidation of indoles/pyrroles using aryl isocyanates mediated by B(C₆F₅)₃. All the reactions were carried out on a 0.1 mmol scale; yields reported are isolated yields.

ESI,† Table S2). Given the presence of unreacted 1*H*-indole starting material in the reaction mixture, we optimised the conditions to improve the yield of **5a** (see ESI,† Table S2).

Scheme 4 Reactivity observed when using 5-bromo-1-methylindole with 4-chlorophenyl isocyanate to afford **2** and **3** (top). Amidation of **1b** using 30 mol% B(C$_6$F$_5$)$_3$ to afford **4** (bottom). All the reactions were carried out on a 0.1 mmol scale; yields reported are isolated yields.

Optimisation of the borane catalyst and conditions revealed that BCl$_3$ (5 mol%) was an efficient catalyst for the *N*-carboxamidation of 1*H*-indole with phenyl isocyanate at 60 °C in 1,2-C$_2$H$_4$Cl$_2$ to afford **5a** in near quantitative yield (93%). The superior reactivity and catalytic property of BCl$_3$ over B(C$_6$F$_5$)$_3$ is attributed to its higher Lewis acidity. From both computational and experimental metrics of Lewis acidity, it can be determined with fair confidence that BCl$_3$ is more Lewis acidic than B(C$_6$F$_5$)$_3$ by Gutmann–Beckett, Childs, and fluoride ion affinity (FIA) measurements.[19,20,21] This can be explained by the increased accessibility of the boron atom in BCl$_3$ upon coordination with a suitable Lewis base, rendering lower strain upon pyramidalisation of the boron centre. Additionally, the global electrophilicity index (GEI) addresses intrinsic Lewis acidity, without dependence on a base, again showing a higher Lewis acidity for BCl$_3$ at 2.077 eV than B(C$_6$F$_5$)$_3$ at 1.408 eV.[22]

Using the optimised reaction conditions of 5 mol% BCl$_3$ in 1,2-C$_2$H$_4$Cl$_2$ at 60 °C, a substrate scope was explored to show the robustness of this methodology (Scheme 5). 1*H*-indole, 5-chloro-1*H*-indole, 3-methyl-1*H*-indole, and 5-methoxy-1*H*-indole were combined with various aryl isocyanates (phenyl isocyanate, *p*-tolyl isocyanate, *p*-chlorophenyl isocyanate, and *p*-methoxyphenyl isocyanate) afford the corresponding urea derivatives in excellent yields (**5a–5k**; yields up to 98%). We further examined the reactivities of carbazole and 1*H*-benzo[*d*]imidazole, towards

phenyl isocyanate. Satisfyingly, excellent yields of the corresponding urea derivatives were again obtained (**5l–5m**, yields up to 97%). Product **5n** was obtained from the reaction between indolin-2-one and phenyl isocyanate in lower yields (48%), presumably due to the strong interaction between the carbonyl functionality and the highly Lewis acidic borane.
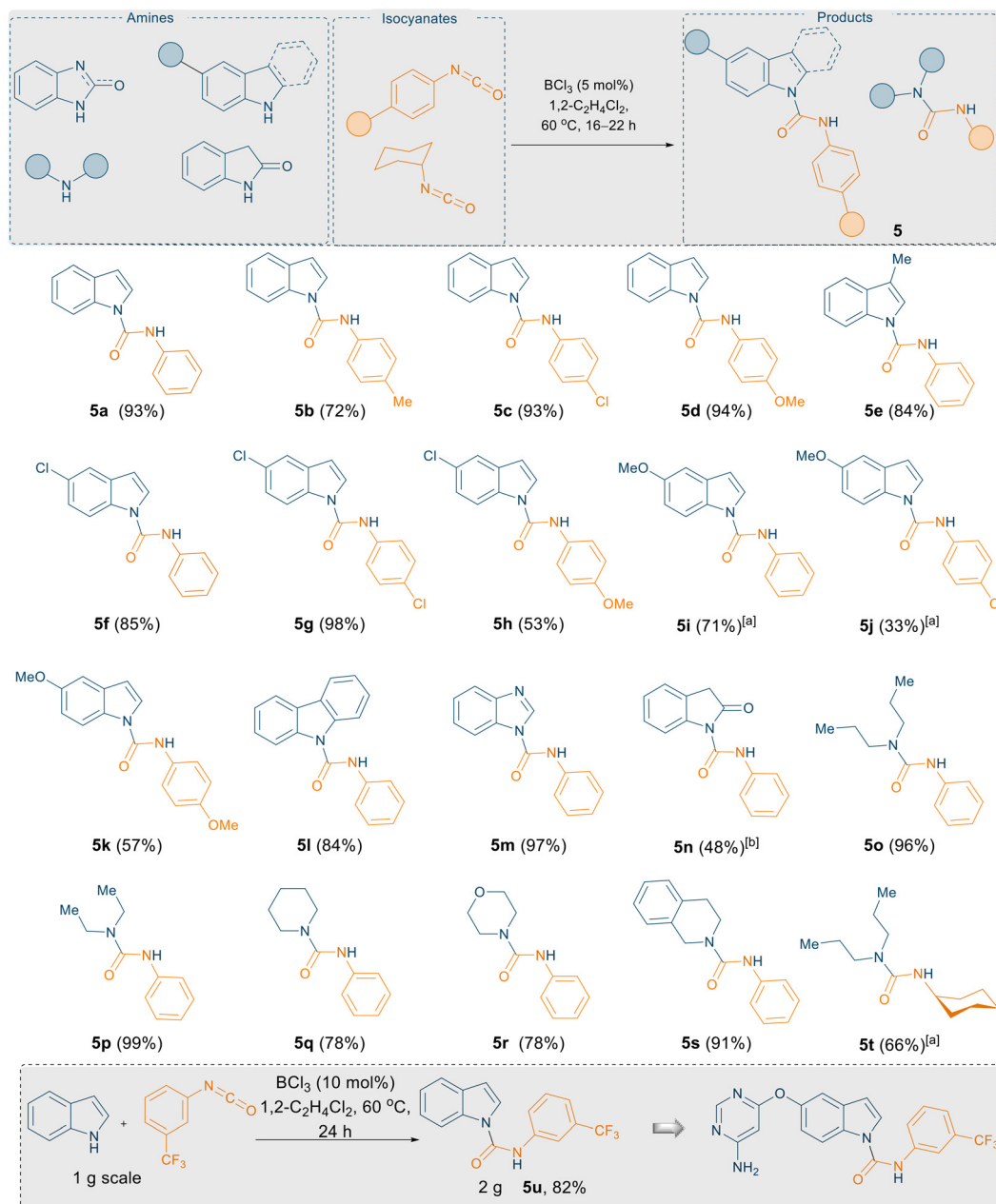
After this successful outcome, we extended the substrate scope to non-aromatic aliphatic secondary amines such as dipropylamine and diethylamine treated with phenyl/cyclohexyl isocyanate. All corresponding urea derivatives (**5o–5t**) were obtained in near quantitative yields (up to 99%). It is noteworthy that in 2017, Bousfield and Camp reported the synthesis of **5o–5s** using bio-alternative solvent cyrene without the aid of any catalyst, albeit in lower yields.[15] For example, the synthesis of **5o** and **5q** are reported in 44% and 61% yields whereas using our optimised catalytic reaction conditions, **5o** and **5q** can be obtained in 98% and 79% yield respectively.

Finally, to demonstrate the utility of this methodology, we employed our procedure towards the synthesis of a core structure of an anti-vascular endothelial growth factor therapeutic compound **5u** (Scheme 5, insert) which is the core structure of a bioactive molecule (Scheme 1, top).[16] A key synthetic step of this oral VEGFR-2 inhibitor was reported using a large excess of NaH (2 equiv.) to couple the isocyanate and indole motifs, or by using 1 mol% copper iodide as a catalyst.[16] Using our slightly modified reaction protocol, the N–H inserted product **5u** could be generated in 82% yield from the reaction of 1*H*-indole with 3-(trifluoromethyl)phenyl isocyanate on gram scale (Scheme 5, insert).

As evidenced from recent literature, 2-alkynyl anilines can undergo an intramolecular cyclisation to afford 2-substituted indoles using catalytic amounts of B(C$_6$F$_5$)$_3$ (5 mol%).[18] We were curious whether an intramolecular hydroamination concept could be applied to generate the indole *in situ* and subsequently substitute the nucleophilic C3 position with an isocyanate to generate the corresponding C3 amides in a one pot reaction. With this target in mind, 2-alkynyl anilines bearing TMS, phenyl, and unsubstituted alkynes were prepared according to literature procedures and employed for the reaction with aryl isocyanates (Scheme 6). Initially, B(C$_6$F$_5$)$_3$ was used (20 mol%) as a catalyst and the reaction was carried out in TFT at 80 °C. A new product was formed and crystallised *via* slow evaporation from CH$_2$Cl$_2$. Single crystal X-ray diffraction data revealed the formation of *N*-carboxamidation product **6a** instead of the expected cyclised-C3-functionalised product (Fig. S132†), which was isolated in 21% yield.

The yield of **6a** was subsequently improved from 21% to 61% by using the optimised reaction conditions for the *N*-carboxamidation of 1*H*-indoles (5 mol% BCl$_3$, 1,2-C$_2$H$_4$Cl$_2$, 60 °C). 2-Alkynyl anilines in combination with various aryl isocyanates selectively afforded the corresponding *N*-carboxamidated products (**6a–6i**, Scheme 6) in good yields (up to 62%).
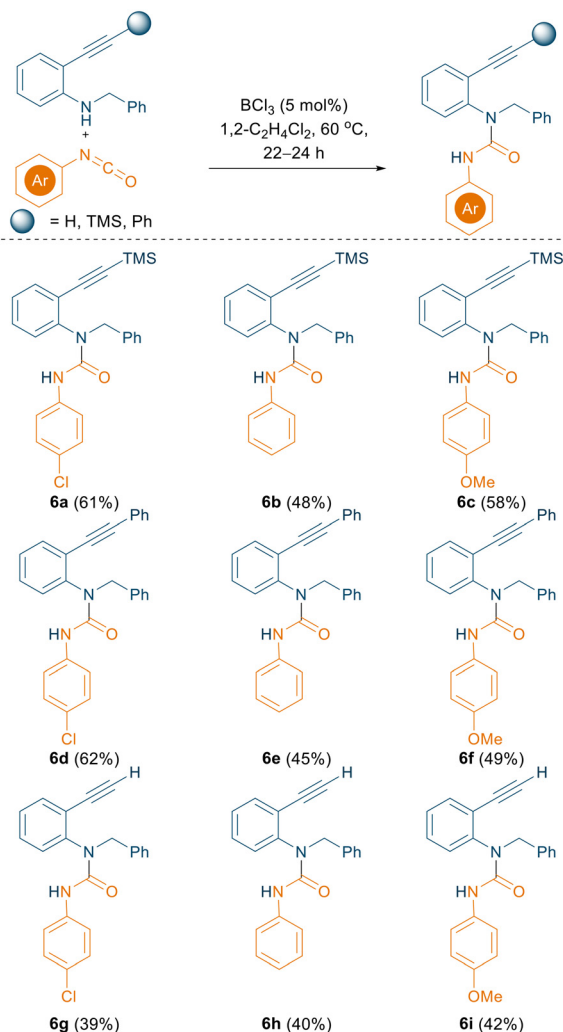
This journal is © The Royal Society of Chemistry 2022

Catal. Sci. Technol., 2022, **12**, 5982–5990 | **5985**

Paper

Scheme 5 BCl$_3$ catalysed N-carboxamidation of 1H-indoles using isocyanates. All the reactions were carried out on a 0.1 mmol scale; yields reported are isolated yields, [a] 10 mol% BCl$_3$ was used, [b] 48 h.

The complete chemo-selectivity observed for unprotected indoles motivated us to establish the most plausible reaction pathway for the N-carboxamidation. We undertook thorough DFT calculations at the SMD/M06-2X/def2-TZVP//SMD/M06-2X/6-31G(d) level of theory in CH$_2$Cl$_2$.

According to the literature, the Lewis acid-catalysed reaction between indole and isocyanate was proposed to take place via two conventional mechanisms depicted in Fig. S134† (cycles A and B). In both cycles the reaction begins with coordination of the acid catalyst to the isocyanate electrophile, thereby activating it towards the nucleophilic attack of the indole. It has been proposed that when

N-protected indoles are used, the catalytic reaction occurs via cycle A, whereas unprotected indoles favour cycle B.[23] To determine the validity of this proposal, we calculated the energy profiles of cycles A and B for the reaction between the unprotected indole and phenyl isocyanate, the results of which are shown in Fig. S134A (left).† In a recent study, we revealed that coordination of BCl$_3$ to the nitrogen atom of isocyanate activates it more effectively than coordination to its oxygen atom.[24] As a result, we only considered this pathway in this work when assuming activation of the isocyanate by BCl$_3$. To begin our computational investigations, we evaluated the stability of various adducts

Scheme 6 BCl_3 catalysed *N*-carboxamidation of 2-alkynyl anilines using aryl isocyanates. All the reactions were carried out on a 0.1 mmol scale; yields reported are isolated yields.

formed by the interaction of BCl_3 with indole and isocyanate. Adduct **7** in which the BCl_3 is bonded to the nitrogen atom of the indole is found to be more stable than the other possible adducts (Fig. S134A,† insert). As a result, adduct **7** is set as the reference structure in all energy profiles calculated in this study.

The calculations for cycle A indicate that nucleophilic attack of the C3 atom of the indole on the BCl_3-activated isocyanate results in the formation of **15**. Once formed, a proton transfer from the C3 atom to the nitrogen atom bonded to BCl_3 yields product **17** while simultaneously regenerating the catalyst BCl_3. As illustrated in Fig. S134† (Cycle A), we used a second indole as a proton transfer agent and determined that this reaction occurs with an overall activation free energy of 23.7 kcal mol^{-1}.

The calculations for cycle B consider the case where the indole acts as a nucleophile attacking the activated isocyanate *via* its nitrogen atom, yielding intermediate **18** (Fig. S134A,† right). The resultant intermediate is then

subjected to a proton transfer process, affording the experimentally observed product **5a** (Fig. S134B,† bottom). According to literature, cycle B should be more favourable than cycle A for unprotected indoles.[23] Contrary to this belief, we found that deprotonation in this pathway *via* transition structure **TS$_9$** requires an activation free energy of 29.7 kcal mol^{-1}, which is higher than the free energies calculated for all transition structures of cycle A (Fig. S134A†). The unfavourable character of this pathway is mainly due to the much lower stability of intermediate **18** compared to its counterpart on cycle A (intermediate **15**). As a result, the formation of product **5a** *via* cycle B is unlikely, and it should be formed *via* a pathway different to those described in previous reports.

After conducting extensive research into an alternative pathway, we identified another cycle (Fig. 2), which accurately accounts for the formation of product **5a** *via* a lower-energy pathway (Fig. 2). Interestingly, the key species in the proposed catalytic cycle is an imine → BCl_3 adduct (**10**·BCl_3) formed by an easy proton transfer process, as described below. As shown in Fig. 2A, the deprotonation of adduct **7** through **TS$_{7-9}$** by another molecule of indole generates iminium ion **8** and the BCl_3-stabilised indolyl anion **9**. Subsequent re-protonation of **9** at the C3 position by **8** yields adduct **10**·BCl_3 through **TS$_{9-10}$**. Our calculations indicate that the formation of adduct **10**·BCl_3 is exergonic with ΔG_{rxn} = −11.0 kcal mol^{-1} and occurs by surmounting an overall activation free energy of 13.5 kcal mol^{-1}. This result implies that in the presence of BCl_3, the indole should initially form adduct **10**·BCl_3, which is the catalyst resting state. It is this species, which reacts with the isocyanate *via* transition state **TS$_{10-12}$** to form intermediate **10**. The relatively high activation free energy of 32 kcal mol^{-1} for the reaction to proceed through catalytic cycle shown in Fig. 2 may be explained by the overestimation of the entropy effect for the bimolecular transformation **10**·BCl_3 + **11** → **TS$_{10-12}$**.[25] The resultant intermediate **12** then undergoes a series of proton transfer processes to form intermediate **13**, with an activation free energy of 9.9 kcal mol^{-1} (Fig. S2†). The formation of the product proceeds through **5a**·BCl_3 and regenerates the catalyst. Adduct **10′** is formed immediately before transition structure **TS$_{10-12}$**. The high basicity of imine **10** results in the corresponding adducts being generated with relative energies of 20.9 (11.3) kcal mol^{-1}. This adduct is highly reactive toward C–N bond formation, yielding **12** by overcoming an activation barrier as low as 0.8 kcal mol^{-1} *via* transition structure **TS$_{10-12}$**. The calculations reveal that although adduct **10′** has lower potential energy than separated structures **10** and **11**, it has higher free energy due to the entropy effect. This explains why **TS$_{10-12}$** and the separated structures **10** and **11** exhibit the same energy trend. The key transition with a relative free energy of 21.7 kcal mol^{-1} is lower in energy than the key transition structures on cycles A and B (see ESI,† Fig. S134), implying that product **5a** is most likely formed *via* this unprecedented mechanism (Fig. 2B). To support our theoretical calculations, we independently
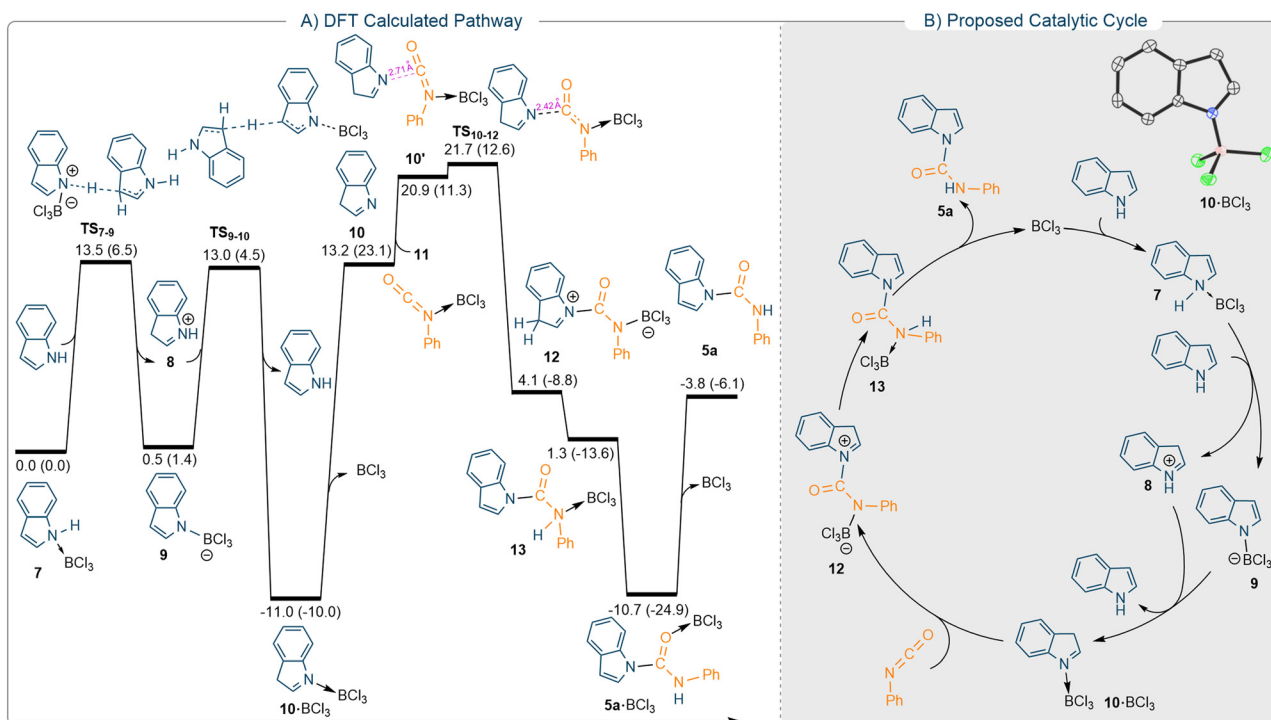
This journal is © The Royal Society of Chemistry 2022

Catal. Sci. Technol., 2022, **12**, 5982–5990 | **5987**

Fig. 2 DFT calculated reaction pathway at the SMD/M06-2X/def2-TZVP//SMD/M06-2X/6-31G(d) level of theory in CH_2Cl_2 for the N-carboxamidation of 1H-indole using phenyl isocyanate and BCl_3 as a catalyst (A). Free energies (potential energies) are given in kcal mol^{-1}. DFT proposed catalytic cycle for the N-carboxamidation of 1H-indole with phenyl isocyanate and catalytic BCl_3 (B). Crystal structure of **10**·BCl_3 (insert, top right). Thermal ellipsoids shown at 50% probability. H atoms omitted for clarity. Carbon: black; nitrogen: blue; chlorine: green; boron: pink.

synthesised the **10**·BCl_3 adduct according to literature procedures[26] and tested it as a catalyst for the reaction. Using the optimised reaction conditions and 5 mol% **10**·BCl_3, the reaction between 1H-indole and phenyl isocyanate showed evidence for formation of **5a** (yield: 75%) as shown by crude ^1H NMR spectroscopy (see ESI,† Fig. S121). A question could be raised that the spontaneous dissociation of **10**·BCl_3 into BCl_3 in solution could potentially catalyse the reaction to afford **5a**. But based on our both experimental and as well DFT calculation data these possibilities can be ruled out. When BCl_3 is released from **10**·BCl_3, the imine **10** is formed, which has a very high nucleophilic character due to its high basicity. This statement is supported by the fact that species **10** can trap BCl_3-activated species **11** with an activation barrier as low as 8.5 kcal mol^{-1} (Fig. 2A). This barrier is lower than the other activation barriers calculated for other chemical steps discussed in this study. This implies that the formation of **5a** is feasible using **10**·BCl_3 as a catalyst. To further validate this claim, two sets of stoichiometric reactions were carried out between **10**·BCl_3/phenyl isocyanate and 1-H indole/phenyl isocyanate/BCl_3. Both reactions afforded the **5a** in a poor yield (approx. 10% calculated from the ^1H NMR spectra of the crude reaction mixture). This can be further justified as the formation of **5a**·BCl_3 is calculated to be an endergonic process with ΔG_{rxn} = +0.3 kcal mol^{-1}. Combining the DFT studies and experimental results, it's clear that the catalytic reaction most likely proceeds *via* the mechanism proposed in Fig. 2B.

Conclusions

In conclusion, a facile metal-free synthetic route has been developed for the amidation of indoles. When using $B(C_6F_5)_3$, N-protected indoles undergo C3 C–H amidation, whereas when using BCl_3, unprotected indoles regioselectively formed N-carboxamidation products in near quantitative yields. A broad substrate scope has been demonstrated to show the wide applicability of the reported methodology. Although 2-alkynyl anilines have been reported to undergo intramolecular hydroamination reactions to afford indole derivatives when using catalytic $B(C_6F_5)_3$, we observed the chemo-selective N-carboxamidation. A detailed mechanistic study revealed the role of the borane catalyst in the initial activation of the indole through imine → BCl_3 adduct formation. This reported methodology furthers the understanding of borane catalysts for metal-free amidation reactions of nitrogen containing heterocyclic compounds.

Experimental

General procedures

A) C3 amidation of indoles. In the glovebox, three glass microwave vials were charged separately with protected indole (1 equiv.), aryl isocyanate (1.5 equiv.), and $B(C_6F_5)_3$ (30 mol%), and were then capped with a septum. The three vials were taken outside the glovebox and 0.5 mL of α,α,α-

5988 | *Catal. Sci. Technol.*, 2022, **12**, 5982–5990

This journal is © The Royal Society of Chemistry 2022

trifluorotoluene (TFT) was added to each vial using a syringe. The RNCO solution was added to the $B(C_6F_5)_3$ solution, and the resulting solution was then added to the indole solution dropwise with vigorous stirring at room temperature. All the reactions were carried out at 80 °C for 22–24 h. All volatiles were removed *in vacuo* and the crude compound was purified *via* preparative thin layer chromatography using hexane/ethyl acetate as eluent.

B) *N*-carboxamidation of indoles. In the glovebox, three glass microwave vials were charged separately with indole (1 equiv.), isocyanate (1.5 equiv.), and BCl_3 [1 M solution in hexane] (5 mol%) and were then capped with a septum. $1,2\text{-}C_2H_4Cl_2$ (0.5 mL) was added to each vial using a syringe outside the glovebox. The isocyanate solution was first added to the BCl_3 solution, and the resulting mixture was then added to the indole solution dropwise with vigorous stirring at room temperature (23 °C). The reaction mixture was heated at 60 °C for 18–24 h. All volatiles were removed *in vacuo* and the crude reaction mixture was purified *via* preparative thin layer chromatography using hexane/ethyl acetate as eluent.

Data availability

ESI includes detailed experimental procedures, NMR spectra, DFT data, and X-ray data. Crystallographic data for **1b**, **1a**·$B(C_6F_5)_3$, **1b**·$B(C_6F_5)_3$, **2**, **3**, **4**, **5a**, **5i**, **5t**, **6a**, and **10**·BCl_3 have been deposited in the Cambridge Crystallographic Data Centre (CCDC) under accession numbers CCDC: 2125082, 2125086, 2125087, 2125085, 2163367, 2143129, 2125083, 2163369, 2167662, 2163272 and 2163368. Information about the data that underpins the results presented in this article, including how to access them, can be found in the Cardiff University data catalogue at **https://doi.org/10.17035/d.2022.0217686022**.

Author contributions

A. D. G. designed and optimised the synthetic method, developed the substrate scope, drafted the manuscript, and directed the project. M. G. G. and N. A. have carried out synthetic work including the reaction optimisations and substrate scope. Y. v. I. undertook X-ray measurements and solved all the crystal structures. A. A. and K. F. carried out the DFT calculations. R. L. M. and E. R. directed the project and wrote the manuscript. All authors analysed the data and proofread the manuscript.

Conflicts of interest

The authors declare no conflict of interest.

Acknowledgements

Notes and references

1 (*a*) L. Li, Z. Wu, H. Zhu, G. H. Robinson, Y. Xie and H. F. Schaefer, *J. Am. Chem. Soc.*, 2020, **142**, 6244–6250; (*b*) R. D. Dewhurst, M. A. Légaré and H. Braunschweig, *Commun. Chem.*, 2020, **3**, 8–11; (*c*) M. A. Légaré, M. Rang, G. Bélanger-Chabot, J. I. Schweizer, I. Krummenacher, R. Bertermann, M. Arrowsmith, M. C. Holthausen and H. Braunschweig, *Science*, 2019, **363**, 1329–1332; (*d*) P. Power, *Nature*, 2010, **463**, 171–177; (*e*) G. C. Welch, R. R. San Juan, J. D. Masuda and D. W. Stephan, *Science*, 2006, **314**, 1124–1126.

2 (*a*) E. Welz, I. Krummenacher, B. Engels and H. Braunschweig, *Science*, 2018, **359**, 896–900; (*b*) K. S. Egorova and V. P. Ananikov, *Angew. Chem., Int. Ed.*, 2016, **55**, 12150–12162.

3 J. Takaya, *Chem. Sci.*, 2021, **12**, 1964–1981.

4 For selected review see: J. L. Carden, A. Dasgupta and R. L. Melen, *Chem. Soc. Rev.*, 2020, **49**, 1706–1725.

5 For a selected review see: (*a*) A. Dasgupta, E. Richards and R. L. Melen, *ACS Catal.*, 2022, **12**, 442–452; also see (*b*) X. Tao, C. G. Daniliuc, R. Knitsch, M. R. Hansen, H. Eckert, M. Lübbesmeyer, A. Studer, G. Kehr and G. Erker, *Chem. Sci.*, 2018, **9**, 8011–8018; (*c*) G.-Q. Chen, G. Kehr, C. G. Daniliuc, M. Bursch, S. Grimme and G. Erker, *Chem. – Eur. J.*, 2017, **23**, 4723–4729; (*d*) I. Chatterjee and M. Oestreich, *Angew. Chem., Int. Ed.*, 2015, **54**, 1965–1968; (*e*) T. Stahl, H. F. T. Klare and M. Oestreich, *ACS Catal.*, 2013, **3**, 1578–1587; (*f*) S. Rendler and M. Oestreich, *Angew. Chem., Int. Ed.*, 2008, **47**, 5997–6000.

6 For selected reviews see: (*a*) D. Maiti, R. Das and S. Sen, *J. Org. Chem.*, 2021, **86**, 2522–2533; (*b*) K. Urbina, D. Tresp, K. Sipps and M. Szostak, *Adv. Synth. Catal.*, 2021, **363**, 2723–2739; (*c*) J. A. Leitch, Y. Bhonoah and C. G. Frost, *ACS Catal.*, 2017, **7**, 5618–5627; (*d*) G. Broggini, E. M. Beccalli, A. Fasana and S. Gazzola, *Beilstein J. Org. Chem.*, 2012, **8**, 1730–1746.

7 For selected reviews on N-heterocycles see: (*a*) D. C. Blakemore, L. Castro, I. Churcher, D. C. Rees, A. W. Thomas, D. M. Wilson and A. Wood, *Nat. Chem.*, 2018, **10**, 383–394; (*b*) E. Vitaku, D. T. Smith and J. T. Njardarson, *J. Med. Chem.*, 2014, **57**, 10257–10274; (*c*) C.-V. T. Vo and J. W. Bode, *J. Org. Chem.*, 2014, **79**, 2809–2815; For selected reviews on indoles see: (*d*) K. Urbina, D. Tresp, K. Sipps and M. Szostak, *Adv. Synth. Catal.*, 2021, **363**, 2723–2739; (*e*) S. Dadashpour and S. Emami, *Eur. J. Med. Chem.*, 2018, **150**, 9–29; (*f*) P. T. Singh and M. O. Singh, *Mini-Rev. Med. Chem.*, 2018, **18**, 9–25.

This journal is © The Royal Society of Chemistry 2022

Catal. Sci. Technol., 2022, **12**, 5982–5990 | **5989**

8 For C3 amidation of indoles using Pd catalyst see: (*a*) J. Peng, L. Liu, Z. Hu, J. Huang and Q. Zhu, *Chem. Commun.*, 2012, **48**, 3772–3774; (*b*) Z. Hu, D. Liang, J. Zhao, J. Huang and Q. Zhu, *Chem. Commun.*, 2012, **48**, 7371–7373; Using Cu catalysts see: (*c*) K. Hirano, T. Satoh and M. Miura, *Org. Lett.*, 2011, **13**, 2395–2397; (*d*) N. Matsuda, K. Hirano, T. Satoh and M. Miura, *J. Org. Chem.*, 2012, **77**, 617–625; Using Rh catalysts see: (*e*) Z. Hu, X. Tong and G. Liu, *Org. Lett.*, 2016, **18**, 2058–2061; Using Zn catalysts see: (*f*) A. Pews-Davtyan and M. Beller, *Org. Biomol. Chem.*, 2011, **9**, 6331–6334; Also see: (*g*) G. Qiu, Q. Ding and J. Wu, *Chem. Soc. Rev.*, 2013, **42**, 5257–5269; (*h*) S. Cacchi and G. Fabrizi, *Chem. Rev.*, 2005, **105**, 2873–2920.

9 K. Nemoto, S. Tanaka, M. Konno, S. Onozawa, M. Chiba, Y. Tanaka, Y. Sasaki, R. Okubo and T. Hattori, *Tetrahedron*, 2016, **72**, 734–745.

10 S. Ye, Q. Ding, Z. Wang, H. Zhou and J. Wu, *Org. Biomol. Chem.*, 2008, **6**, 4406–4412.

11 J. Chen, L. Hu, H. Wang, L. Liu and B. Yuan, *Eur. J. Org. Chem.*, 2019, **2019**, 3949–3954.

12 N. Pannilawithana and C. S. Yi, *ACS Catal.*, 2020, **10**, 5852–5861.

13 T. Jeong, S. Han, N. K. Mishra, S. Sharma, S. Y. Lee, J. S. Oh, J. H. Kwak, Y. H. Jung and I. S. Kim, *J. Org. Chem.*, 2015, **80**, 7243–7250.

14 W. Yan, W. Shan, Z. Hailing, C. Rui and H. Shuhua, *Chin. J. Org. Chem.*, 2019, **39**, 3567–3573.

15 L. Mistry, K. Mapesa, T. W. Bousfield and J. E. Camp, *Green Chem.*, 2017, **19**, 2123–2128.

16 E. L. Meredith, N. Mainolfi, S. Poor, Y. Qiu, K. Miranda, J. Powers, D. Liu, F. Ma, C. Solovay, C. Rao, L. Johnson, N. Ji, G. Artman, L. Hardegger, S. Hanks, S. Shen, A. Woolfenden, E. Fassbender, J. M. Sivak, Y. Zhang, D. Long, R. Cepeda, F. Liu, V. P. Hosagrahara, W. Lee, P. Tarsa, K. Anderson, J. Elliott and B. Jaffee, *J. Med. Chem.*, 2015, **58**, 9273–9285.

17 M. Nakamura, L. Ilies, S. Otsubo and E. Nakamura, *Org. Lett.*, 2006, **8**, 2803–2805.

18 S. Tussing, M. Ohland, G. Wicker, U. Flörke and J. Paradies, *Dalton Trans.*, 2017, **46**, 1539–1545.

19 (*a*) P. Erdmann and L. Greb, *Angew. Chem., Int. Ed.*, 2022, DOI: **10.1002/anie.202114550**; (*b*) R. J. Mayer, N. Hampel and A. R. Ofial, *Chem. – Eur. J.*, 2021, **27**, 4070–4080; (*c*) I. B. Sivaev and V. I. Bregadze, *Coord. Chem. Rev.*, 2014, **270–271**, 75–88.

20 (*a*) I. B. Sivaev and V. I. Bregadze, *Coord. Chem. Rev.*, 2014, **270–271**, 75–88; (*b*) R. F. Childs, D. L. Mulholland and A. Nixon, *Can. J. Chem.*, 1982, **60**, 809–812.

21 P. Erdmann, J. Leitner, J. Schwarz and L. Greb, *ChemPhysChem*, 2020, **21**, 987–994.

22 (*a*) A. R. Jupp, T. C. Johnstone and D. W. Stephan, *Inorg. Chem.*, 2018, **57**, 14764–14771; (*b*) A. R. Jupp, T. C. Johnstone and D. W. Stephan, *Dalton Trans.*, 2018, **47**, 7029–7035.

23 B. Yuan, J. Wan, X. Guo, Y. Gong, F. Zhang, Q. Li, G. Wang, J. Chen and R. He, *New J. Chem.*, 2020, **44**, 9878–9887.

24 A. Dasgupta, Y. van Ingen, M. Guerzoni, K. Farshadfar, J. M. Rawson, E. Richards, A. Ariafard and R. L. Melen, *Chem. – Eur. J.*, 2022, DOI: **10.1002/chem.202201422**.

25 The relatively high activation free energy of 32 kcal mol^{-1} for the reaction to proceed through catalytic cycle shown in Fig. 2 may be explained by the overestimation of the entropy effect for the bimolecular transformation **10**·BCl$_3$ +**11** → **TS$_{10-12}$**.

26 S. Guidotti, I. Camurati, F. Focante, L. Angellini, G. Moscardi, L. Resconi, R. Leardini, D. Nanni, P. Mercandelli, A. Sironi, T. Beringhelli and D. Maggioni, *J. Org. Chem.*, 2003, **68**, 5445–5465.

5990 | *Catal. Sci. Technol.*, 2022, **12**, 5982–5990

This journal is © The Royal Society of Chemistry 2022